

PAPER • OPEN ACCESS

## Identification of damages in a concrete beam: a modal analysis based method

To cite this article: G. Cosoli *et al* 2024 *J. Phys.: Conf. Ser.* **2698** 012014

View the [article online](#) for updates and enhancements.

You may also like

- [Belarusian \*in utero\* cohort: A new opportunity to evaluate the health effects of prenatal and early-life exposure to ionising radiation](#)  
Vasilina Yauseyenko, Vladimir Drozdovitch, Evgenia Ostroumova et al.
- [Guiding principle for crystalline Si photovoltaic modules with high tolerance to acetic acid](#)  
Atsushi Masuda and Yukiko Hara
- [An abrasive wear test for thin and small-sized steel blade specimens](#)  
N Mahathaninwong, T Chucheep, S Janudom et al.

**PRIME**  
PACIFIC RIM MEETING  
ON ELECTROCHEMICAL  
AND SOLID STATE SCIENCE

HONOLULU, HI  
Oct 6-11, 2024

Abstract submission deadline:  
**April 12, 2024**

Learn more and submit!

**Joint Meeting of**  
The Electrochemical Society  
•  
The Electrochemical Society of Japan  
•  
Korea Electrochemical Society

# Identification of damages in a concrete beam: a modal analysis based method

G. Cosoli<sup>1</sup>, M. Martarelli<sup>1</sup>, A. Mobili<sup>2</sup>, F. Tittarelli<sup>2,3</sup>, G.M. Revel<sup>1</sup>

<sup>1</sup> Department of Industrial Engineering and Mathematical Sciences, Università Politecnica delle Marche, v. Breccie Bianche snc, 60131 Ancona (Italy)

<sup>2</sup> Department of Materials, Environmental Sciences and Urban Planning, Università Politecnica delle Marche, v. Breccie Bianche snc, 60131 Ancona, Italy

<sup>3</sup> Institute of Atmospheric Sciences and Climate, National Research Council (ISAC-CNR), v. Gobetti 101, 40129 Bologna, Italy

g.cosoli@staff.univpm.it, 0000-0001-7982-208X

**Abstract.** Structural Health monitoring (SHM) strategies can play a pivotal role in the perspective of enhancing structures and infrastructures life cycle and maintenance operations. A plethora of sensors and technologies can be employed in this field; in a seismic context, vibrational tests are particularly relevant, being able to give an insight on the dynamic characteristics of the structure itself. In particular, modal parameters can be considered in order to detect damages. A comparison between a certain test time and 0 test time (i.e., undamaged structure) is commonly performed; to this aim numerical models result particularly useful to provide baseline data (often unavailable in pre-existing structures), but they need to be validated before use. Non-contact techniques, like scanning laser Doppler vibrometry, can be exploited to do this. In this paper a numerical model of a scaled concrete beam is realized and validated through LDV data, then it is used to design load tests for progressive damages generation. Modal analysis is conducted after different load trials to evaluate changes of modal parameters in relation to the damage occurred; also, damage-related indices are proposed. The results confirmed the suitability of LDV for dynamic analyses of cement-based structures and this can be particularly useful when big structures (e.g., bridges) have to be monitored in-field. The numerical model was validated with acceptable absolute errors in terms of natural frequencies (between 26 Hz and 131 Hz) and high Modal Assurance Criterion (MAC) values (0.85-0.93). Moreover, the proposed methodology allows to detect damages also in a concise way through synthetic indices (with changes >50% in damaged vs undamaged conditions) and early warnings could be generated according to their values, hence supporting decision-making procedures in the building management scenario.

## 1. Introduction

Structural Health Monitoring (SHM) techniques can play a pivotal role in the optimization of a structure/infrastructure life cycle as well as of interventions costs. Indeed, monitoring a building with appropriate sensors and regularly checking the gathered data from remote gives the possibility to promptly detect any issue, possibly due to abnormal external loads or penetration of contaminants. In this context, Internet of Things (IoT) enabled technologies eases data transfer (e.g., on Cloud-based services) and, hence, remote monitoring possibilities [1]. Different types of sensors and technologies



can be exploited for SHM purposes, such as strain gages, load cells, accelerometers, electrical impedance sensors, and vision-based systems [2–4]. In last decades also Artificial Intelligence (AI) based methods have been employed, when big data are available [5].

If we consider seismic areas, vibrational tests have a particular relevance, since they can provide an insight on the dynamical behavior of the structure itself. When an earthquake occurs, it is fundamental to timely identify damages (especially when occurring in critical structures, e.g., hospitals, fire and police stations, etc.) and intervene as soon as possible, optimizing the interventions effectiveness as well as costs. Monitoring strategies undoubtedly overcome inspections in this case, especially when an early warning system is present.

Also, non-contact techniques, such as laser Doppler vibrometry (LDV), have been demonstrated to be very effective for defects identification. They can be particularly useful when a large structure has to be monitored and the installation of multiple hardware sensors would be very difficult, cumbersome, and also expensive. Sugimoto et al. [6] exploited LDV to detect internal defects of concrete by analyzing resonance frequencies. LDV was used by Zhao et al. [7] to estimate and characterize debonding areas on tiles. Liarakos et al. [8] applied laser scanner vibrometry to map structural damages in concrete specimens and evidenced discontinuities in the velocity signal linked to the presence of cracks. Zhao et al. [9] combined vibration measurements and a convolutional neural network (CNN) to identify defects on a beam; this procedure could potentially be employed for real-time diagnosis. Also Muramatsu et al. [10] used a CNN to detect cracks through the analysis of vibration data acquired by means of LDV, achieving an accuracy higher than 90% but also highlighting that experimental data are more hard to interpret with respect to those obtained through numerical simulations on finite element method (FEM) models. Indeed, in order to extract as much information as possible from experimental LDV measured signals, specific data processing techniques can be applied, such as Continuous Wavelet Transform (CWT) [11].

This work aims at employing LDV to validate a numerical model representing a concrete scaled beam (1:5) to be subjected to modal analysis. Once validated, the model was used to plan experimental tests for damage identification through experimental modal analysis considering Inertance. These activities were performed within the reCITY project (Resilient City – Everyday Revolution – PON R&I 2014-2020 e FSC “Avviso per la presentazione di Ricerca Industriale e Sviluppo Sperimentale nelle 12 aree di Specializzazione individuate dal PNR 2015-2020”, identification code ARS01\_00592), which aims at realizing a community-centred social, economic, and technological system to valorise resilience practices, supporting the whole community in emergency situations. In particular, within the framework of this project Università Politecnica delle Marche develops measurement strategies to support the management of critical infrastructures in a post-seismic context. Specifically, a monitoring network based on innovative sustainable materials – also with self-sensing/monitoring capabilities – and distributed sensors was realised. Modal analysis is exploited to identify the presence of damages through the evaluation of changes in terms of modal parameters (i.e., natural vibration frequency and loss factor), mode shapes and related modal curvatures, as well as to define damage-related indices providing synthetic information on the structural health status, in order to support decision-making processes in a seismic context.

The remainder of the paper is organised as follows: Section 2 describes the materials and methods of the study, the results are reported and discussed in Section 4. Finally, the authors draw their conclusions and provide final considerations in Section 5.

## 2. Materials and methods

The materials and methods followed for the present study are reported in this section.

### 2.1. Concrete specimen manufacturing process

At first, the authors manufactured a concrete beam (10 cm x 10 cm x 50 cm) according to the mix-design reported in Table 1. Portland cement (CEM II/A-LL 42.5R) was employed, together with a calcareous sand (0-8 mm). The water/cement (w/c) ratio was equal to 0.50 by mass, hence achieving a

S5 workability class (the tests were performed through the Abrams cone). Carbon-based additions were inserted in the mix-design, in order to enhance the material self-sensing and monitoring capabilities (which can be exploited through electrical impedance measurements, but this goes beyond the scope of this work). In particular, the following conductive additions were selected:

- recycled carbon fibres (RCF, Procotex Belgium SA, Belgium).
- carbonaceous filler, i.e., biochar (BCH, RES – Reliable Environmental Solutions, Italy).

The choice was based on a previous research activity, performed within the European H2020 project EnDurCrete (GA n. 760639), which led to the patent n. 10202000022024 titled “Eco-compatible and self-sensing mortar and concrete compositions for manufacturing reinforced and non-reinforced constructive elements, related construction element and methods for the realization of self-monitorable building structures”.

**Table 1.** Mix-design of the concrete scaled beam.

Cement [kg/m <sup>3</sup> ]	Water [kg/m <sup>3</sup> ]	Air [%]	Sand [kg/m <sup>3</sup> ]	Intermediate gravel [kg/m <sup>3</sup> ]	Coarse gravel [kg/m <sup>3</sup> ]	RCF [kg/m <sup>3</sup> ]	BCH [kg/m <sup>3</sup> ]
470.0	235.0	2.5	795.0	321.0	476.0	0.9	10.0

## 2.2. FEM model and numerical simulation

A FEM model of the scaled beam was realized, including all the sensors and components present in the real specimen. The geometry (**Figure 1**) includes the following elements:

- Embedded sensors for SHM (beyond the scope of this work).
- Lateral plastic tubes for electric cables (clearly influencing modal parameters).
- Metallic plates, acting as bases for accelerometers positioning.
- DOFs for LDV signal (n. 60).

The numerical simulation was run in COMSOL® Multiphysics environment. In particular, the Structural Mechanics Module was employed and the Eigenfrequency study was performed considering free-free conditions (i.e., the structure is not constrained). The results were evaluated in terms of both natural frequencies and mode shapes.

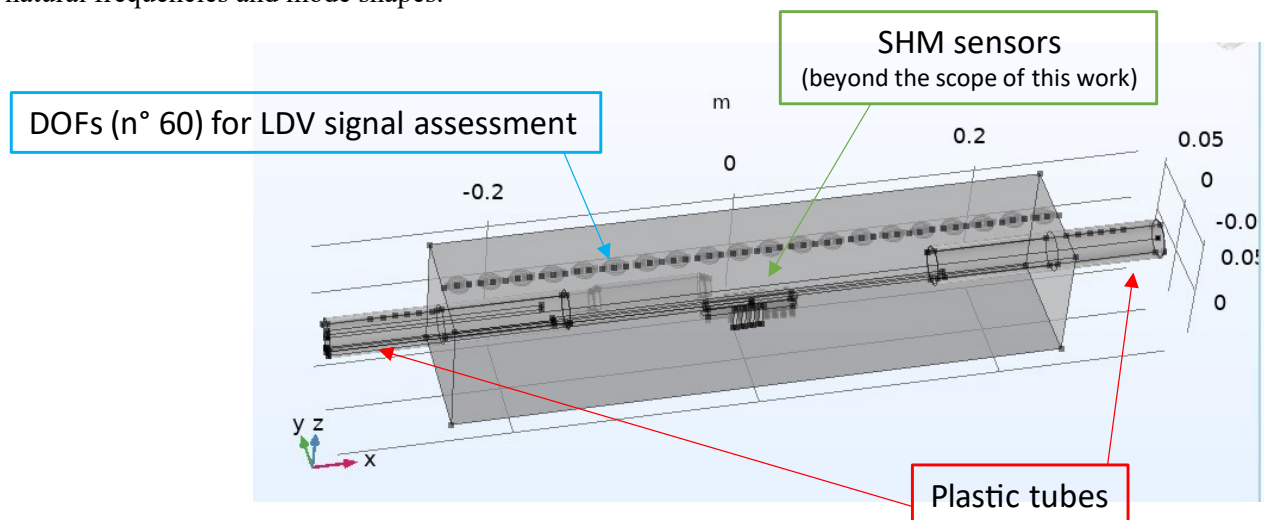


**Figure 1.** Geometry of the FEM model.

Before being exploitable, the model needed to be validated; scanning LDV was employed to this aim (Section 2.3). Hence, the model was used to design load tests on the real concrete beam (Section 2.4) aiming at damage identification through vibrational tests (Section 2.5) and modal analysis (Section 2.6).

### 2.3. Model validation

The FEM model was validated through an experimental setup including a scanning LDV (PSV-500, Polytec GmbH, Germany – **Figure 2**). The laser head was positioned perpendicular to the specimen surface and the beam focus was optimized at each acquisition point (a 45% zinc oxide hydrating lotion was applied on the surface to enhance the signal quality). A linear grid with 60 scanning points was defined and the velocity signal was acquired for each of them, in order to define the dynamic response of the structural element with respect to the excitation provided by the impact hammer on the driving point (located on the specimen midline).

### 2.4. Load tests

The load tests were composed of multiple trials involving different load levels, progressively leading to the fracture of the specimen and to the enlargement of the crack aperture. A mechanical press (Zwick Roell, maximum load: 600 kN) was used to apply the load at the center of the concrete specimen, positioned on two pins distanced 30 cm from each other (Figure 3).

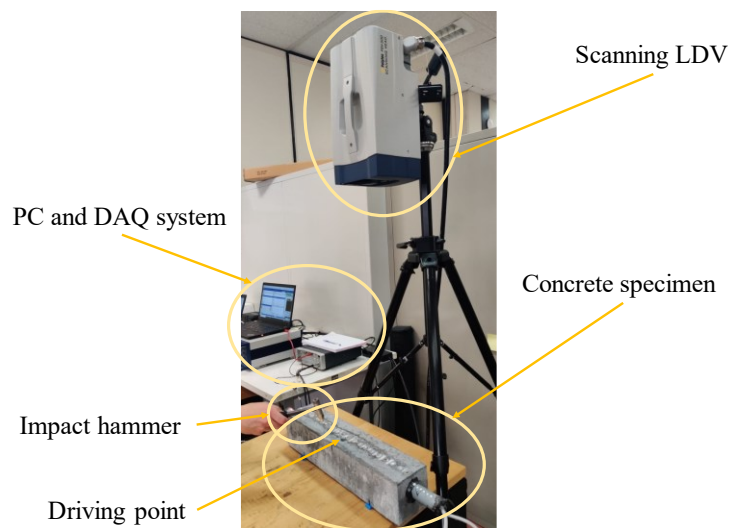


**Figure 2.** Experimental setup with scanning LDV for FEM model validation.

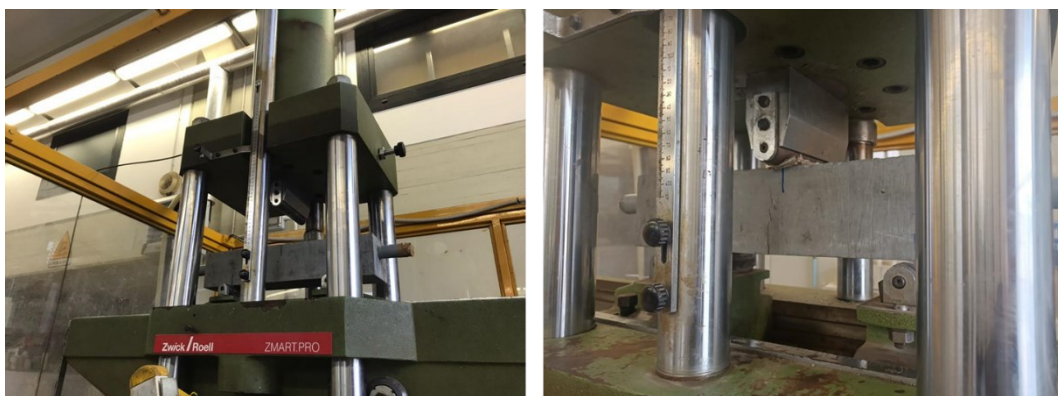


**Figure 3.** Experimental setup for load tests: concrete specimen positioning (left) and load application (right).

The concrete beam was subjected to 3 increasing level loads:

1. 90% of the fracture load (t1).
2. Fracture load (t2).
3. Load at which the crack aperture is approximately 1 mm (t3).



In this way, progressive cracking phenomena were caused.

After each load trial (and before loading the specimen, test time  $t_0$ ), a vibrational test was carried out, as described in detail in the next section.

### 2.5. Vibrational tests

After each load trial, a vibrational analysis was performed (**Figure 4**).



**Figure 4.** Vibrational tests execution: accelerometers installation (left) and structure excitation with impact hammer (right).

The concrete element was excited using an impact hammer and the corresponding dynamic response was assessed by means of piezoelectric accelerometers (measuring on  $z$  axis) positioned in 20 equally spaced degrees of freedom (2.5 cm from each other), as reported in Figure 5. A total of 5 accelerometers were employed in rowing mode, hence 4 subsequent sessions were necessary to scan the whole specimen. Data were acquired through the LMS SCADAS Mobile (Siemens); the frequency range was 0-4096 Hz with a 0.25 s test duration. Five repeated acquisitions on each DOF were performed to enhance the Signal-to-Noise Ratio (SNR).

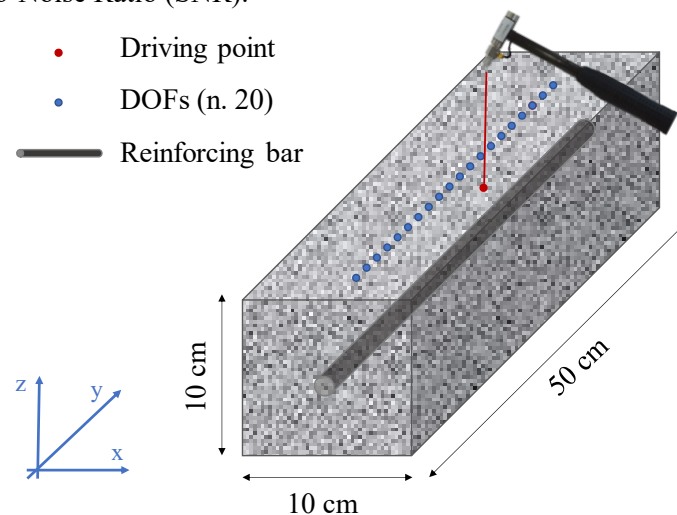


**Figure 5.** Reinforced concrete specimen with indication of driving point and DOFs.

The experimental results in terms of natural vibration frequencies and mode shapes (measured on the intact specimen as described in detail in the next section) were compared to the numerical ones to

validate the numerical model. Also, the Modal Assurance Criterion (MAC) was applied to evaluate the correlation between numerical and experimental results.

### 2.6. Damage identification procedure

A damage identification procedure was defined thanks to experimental modal analysis, modal curvature computation, and CWT-based analysis. Specifically, modal analysis was performed within Simcenter Testlab software (Siemens PLM, Texas, US). The inertance was considered (accelerometers were employed to measure the dynamical response of the system) and the rigid-body, I, and II mode shapes of the concrete beam were analysed. Both natural frequency ( $f_n$  [Hz]) and loss factor ( $\eta$  [%]) were computed; their changes at different load levels were evaluated, being them related to structural integrity [12,13]. Also, the modal curvatures were computed to highlight the changes due to the damage occurrence [14]. Hence, an analysis based on CWT was conducted to evidence these modifications in case of damage occurrence.

Finally, three damage related indices were synthesized to characterize both the occurrence and the severity of a damage.

Three damage-related indices were proposed:

- $DI_{curv}$  (1): it considers the differences of modal curvature at a certain test time  $x$  ( $\varphi''_{tx}$ ) with respect to the initial conditions (i.e., intact specimen,  $t_0$ ,  $\varphi''_{t_0}$ ) – it recalls the Curvature Damage Factor, CDF, introduced by Pranno et al. [15]. Each difference is normalised to the maximum value of the curvature at  $t_0$  (i.e.,  $\max|\varphi''_{t_0}|$ ). It is expected to increase with damage, since curvatures change their morphology with respect to intact condition.

$$DI_{curv} = \sum_{i=1}^N \frac{|\varphi''_{tx} - \varphi''_{t_0}|}{\max|\varphi''_{t_0}|} \quad (1)$$

- $DI_{CWT}$  (2): it is derived from the CWT-based analysis. In particular, the image obtained through the application of CWT was binarized (automatic threshold defined with the Otsu's method [48]) and the area of high coefficients were calculated at a determined test time  $tx$  (i.e.,  $\sum_{i=1}^N (pixel = 1)|_{tx}$ ). The value was normalised with respect to the area obtained at  $t_0$  test time (i.e.,  $\sum_{i=1}^N (pixel = 1)|_{t_0}$ ). It should decrease when damage occurs, since there is the formation of a cuspid.

$$DI_{CWT} = \frac{\sum_{i=1}^N (pixel = 1)|_{tx}}{\sum_{i=1}^N (pixel = 1)|_{t_0}} \quad (2)$$

- $DI_{global}$  (3): it is a combination of the two previously introduced indices. Hence, it is assumed to increase with damage.

$$DI_{global} = \frac{DI_{curv}}{DI_{CWT}} \quad (3)$$

All the indices were evaluated on the modal curvature related to the I mode shape of the beam, which is the most sensitive to damage occurrence.

### 3. Results and discussion

The damage occurrence can be evidenced by multiple effects on the dynamical characteristics of the concrete element, namely:

- Natural frequency decrease: this is attributable to the rigidity loss of the material.

- Loss factor increases, due to stiffness decrease.
- Appearance of a cuspid in the I mode shape of the beam, highlighted in the related modal curvature. This is linked to the fact that the crack forms in the midline of the specimen, which actually divides into two halves vibrating almost separately as the crack aperture increases.

The results of the numerical model, of experimental tests, and of experimental damage detection are reported in detail in the next sections.

### 3.1. Numerical model

Three main mode shapes were identified:

- A first mode shape related mainly to tubes, moving in a synchronous way (Figure 6).
- A second mode shape related mainly to tubes, moving in an asynchronous way (Figure 7).
- A third mode shape proper of the concrete beam (which is the I mode shape typical of a beam in free-free conditions – Figure 8).

The natural frequencies of the three modes are 1117 Hz, 1447 Hz, and 1675 Hz, respectively.

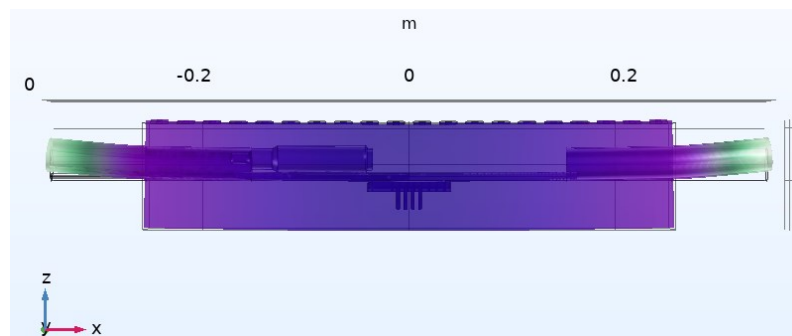


**Figure 6.** First mode shape, acceleration, z-component (tubes, synchronous movement).

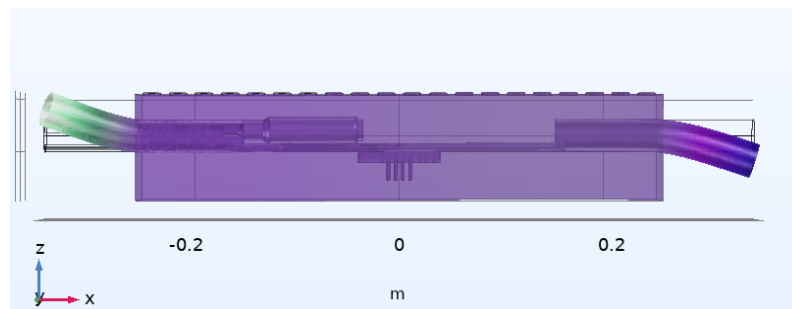


**Figure 7.** Second mode shape, acceleration, z-component (tubes, asynchronous movement).

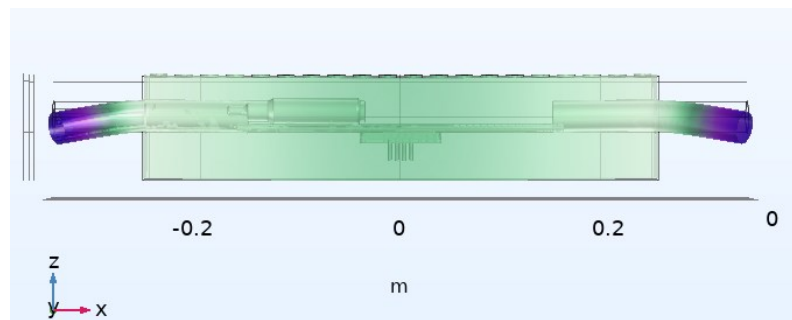


**Figure 8.** Third mode shape, acceleration, z-component (beam - I mode shape typical of a beam in free-free conditions).



Indeed, it is worthy to note that also in the mode shapes linked to the external tubes the beam vibrates, but the vibrations amplitude is moderate with respect to the tubes one.

### 3.2. Comparison between numerical and experimental results

In order to validate the numerical model, a comparison with the experimental results obtained from the LDV measurements was performed. The modal parameters calculated with the numerical model were compared with the ones estimated via modal analysis on the basis of the Frequency Response Functions (FRFs) dataset measured with the scanner LDV. Modal analysis was performed by means of the Simcenter Testlab Modal Analysis tool in frequency domain by applying the PolyMAX algorithm. The comparison in terms of both mode shape and natural vibration frequency is reported in **Figure 9** for the first mode (tubes vibration, synchronous), in **Figure 10** for the second mode (tubes vibration, asynchronous), and **Figure 11** for the third mode (beam vibration). In the experimental model there are electric cables exiting the left tube, hence that side is more rigid (thus, movements will be more limited than the right side).

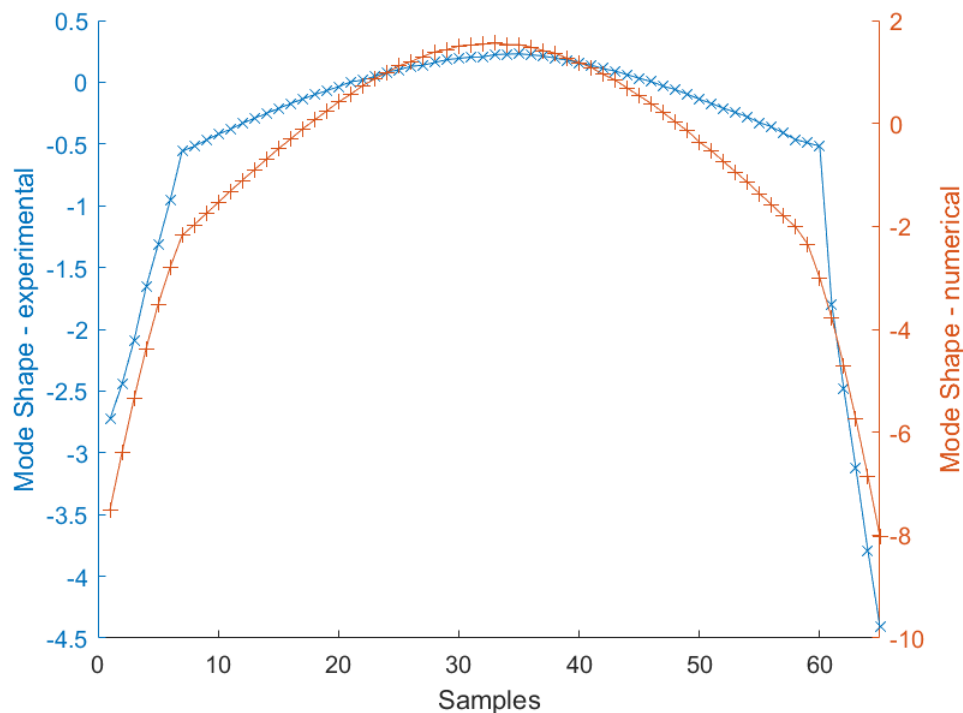


**Figure 9.** Numerical (red –  $f_n = 1117$  Hz) and experimental (blue –  $f_n = 1143$  Hz) results comparison - first mode shape (tubes vibration, synchronous).

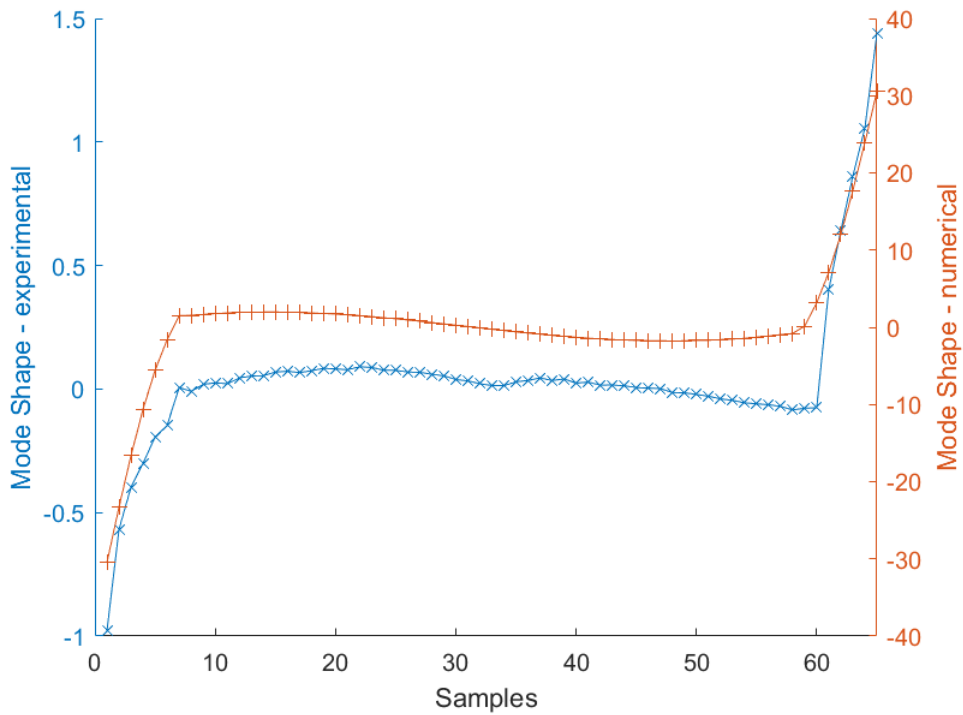


**Figure 10.** Numerical (red –  $f_n = 1447$  Hz) and experimental (blue –  $f_n = 1316$  Hz) results comparison - second mode shape (tubes vibration, asynchronous).

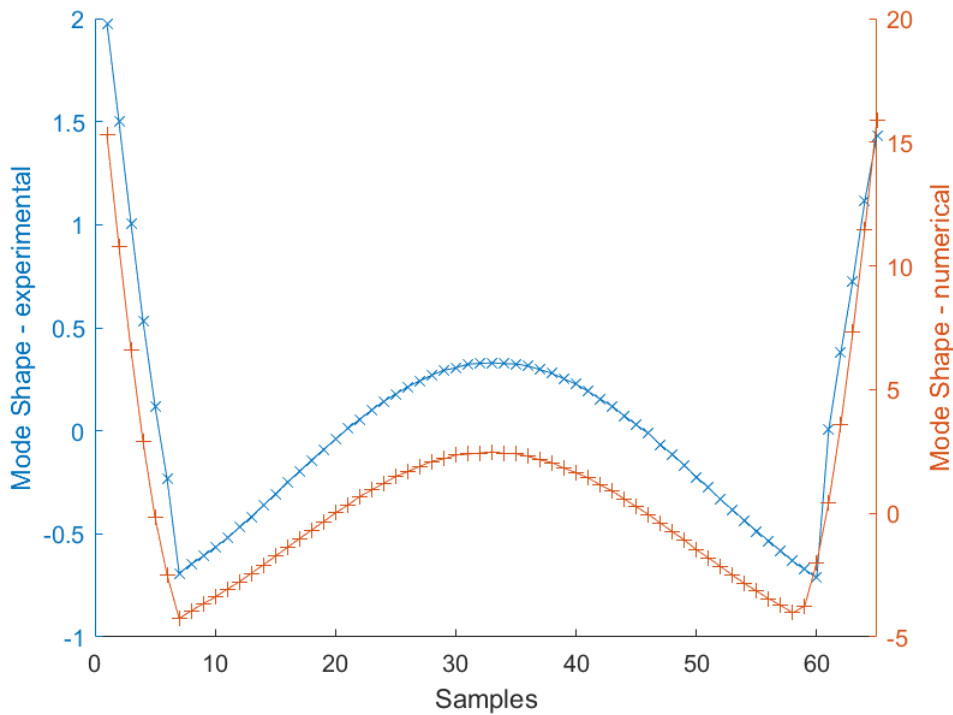


**Figure 11.** Numerical (red –  $f_n = 1675$  Hz) and experimental (blue –  $f_n = 1637$  Hz) results comparison - third mode shape (beam vibration).

The comparison was very good, reporting a MAC between 0.85 and 0.93 (**Table 2**). Some discrepancies can be attributed to the fact that in the experimental setup there are cables exiting one of the two external plastic tubes, making that side more rigid. The absolute error in terms of natural vibration frequencies was between 26 Hz and 131 Hz (**Table 2**). This is acceptable, given the high intrinsic variability of cement-based materials and, hence, the plausible discrepancies between the numerical model and the real concrete specimen.

**Table 2.** Comparison between numerical and experimental model.

Mode	Experimental $f_n$ [Hz]	Numerical $f_n$ [Hz]	MAC
I (tubes)	1143	1117	0.89
II (tubes)	1316	1447	0.85
III (I beam mode)	1637	1675	0.93

### 3.3. Damage detection

For damage detection, the first two main mode shapes typical of a beam in free-free conditions were considered (**Figure 12**). For the sake of clarity, it is worthy to underline the fact that the I mode shape of the beam (**Figure 12**, top) corresponds to the third mode shape identified in the numerical model (**Figure 8**). These were evaluated at each test time (i.e.,  $t_0$ ,  $t_1$ ,  $t_2$ , and  $t_3$ ), in order to highlight the changes with respect to the initial condition (i.e.,  $t_0$ , intact specimen).

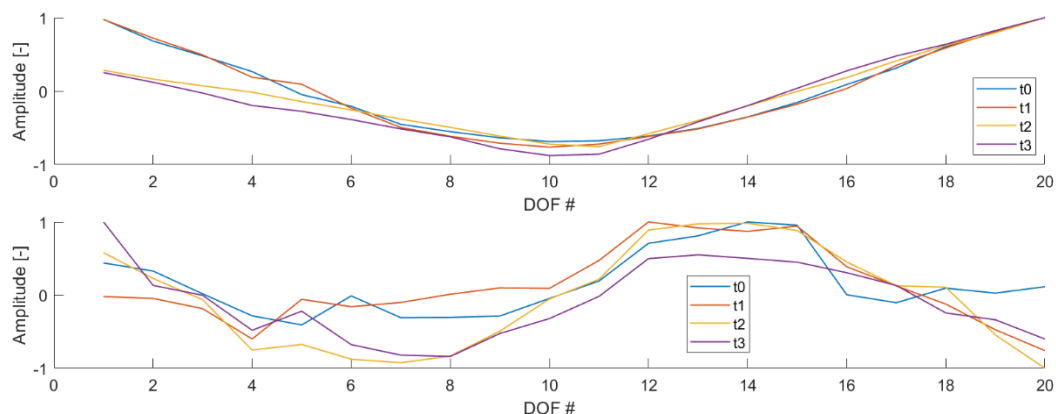


**Figure 12.** Experimental I (top) and II (bottom) mode shapes of the concrete beam at each test time.

When a damage occurs (i.e., a crack forms, from  $t_2$  onwards), it is possible to notice both a decrease in terms of natural frequency (**Figure 13**) and an increase in the loss factor (**Figure 14**), both due to the stiffness decrease of the material itself. Natural vibration frequency significantly decreases when the first crack appears (i.e., at  $t_2$  test time), whereas the change between  $t_0$  and  $t_1$  and between  $t_2$  and  $t_3$  is not so marked; in fact, at  $t_1$  the structural element should not be damaged yet, given that the applied load is lower than its mechanical resistance. Concerning the loss factor, as expected its changes are not so easy to be accurately identified; however, an increasing trend can be recognized over the trial, following the progressive degradation of the material. The only exception is at  $t_1$  for the I mode shape, otherwise the other points are in line with what expected. Observing the I mode shape of the beam (**Figure 12**, top), it is possible to identify the appearance of a cuspid in correspondence of the damage location (in the specimen midline, i.e., close to the DOF n. 10); this feature can be evidenced in the related modal curvature, especially if specific data processing techniques are applied, such as CWT (**Figure 15**). The cuspid formation is clear at  $t_2$  test time and becomes also more marked at  $t_3$ , when the

crack aperture is enlarged (approximately up to 1 mm). However, it is worthy to note that all the assessments were made after the load removal, hence a partial closure of the crack occurred.

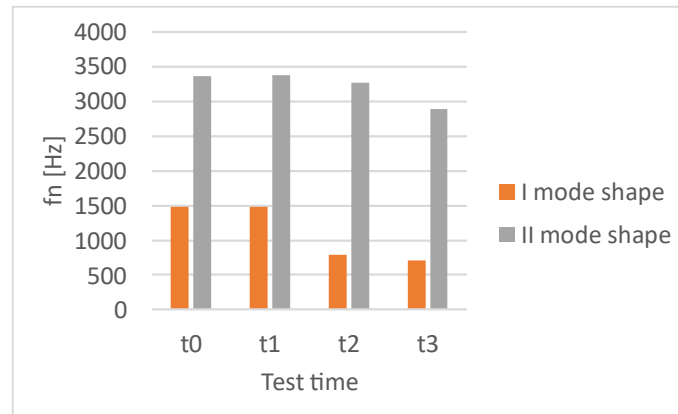


**Figure 13.** Changes in terms of natural vibration frequencies in I and II mode shapes of the beam at different test times.

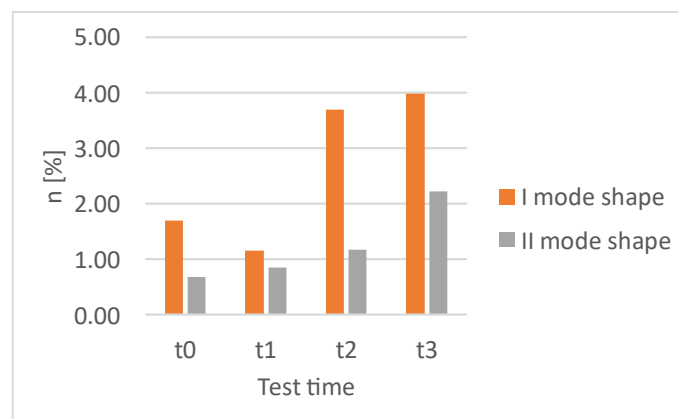


**Figure 14.** Changes in terms of loss factor in I and II mode shapes of the beam at different test times.

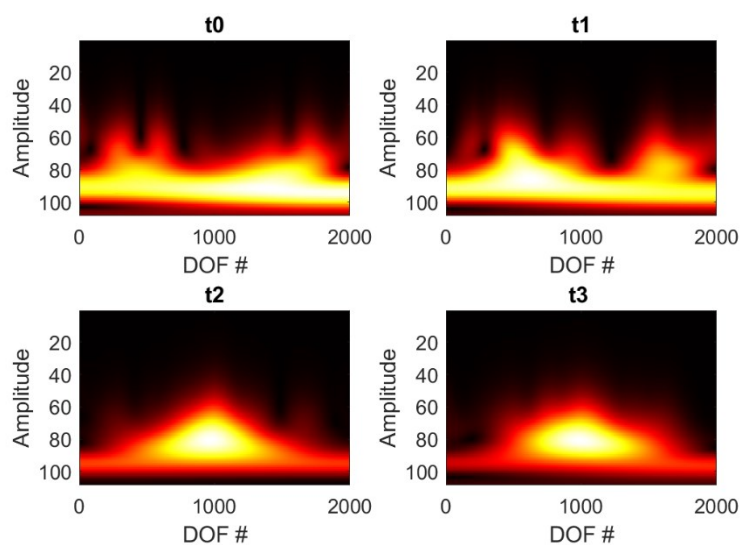


**Figure 15.** Results of CWT-based analysis (I modal curvature).

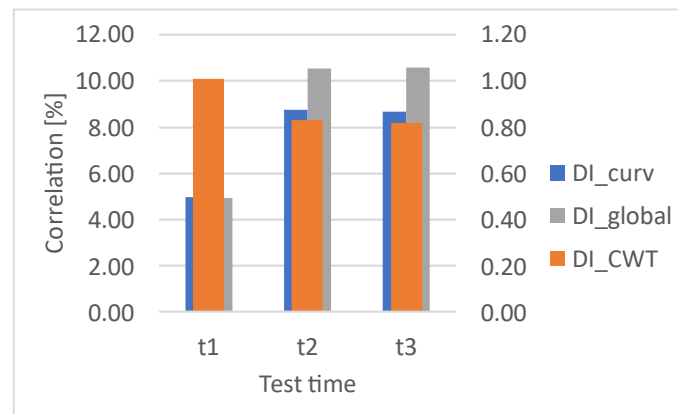


**Figure 16.** Damage related indices at different test times.

#### 4. Conclusions

Modal-based analysis applied on a concrete beam confirmed to be effective for damage identification, especially when combined to specific data processing techniques (CWT). Synthetic damage indices can help in describing a concrete element concerning structural health status, allowing to locate damages and to assess their severity. The regular evaluation of such indices can help organizing the maintenance activities in a view of life cycle optimization and early warnings generation. This allows to optimize both interventions and costs for the management of a structure or an infrastructure. However, to make such indices more reliable and precise, a wider experimental campaign should be conducted, considering also different operating conditions and different types of damages.

The methodologies for damage identification in this context are often based on the comparison of modal parameters at a certain test time with those obtained in the initial conditions. However, in a pre-existing structure this information could not be available. Hence, numerical models can support the procedure by providing the modal parameters on the intact structural element (i.e., the baseline data). To obtain reliable and accurate results, such models need to be properly validated before application. This can be done through dedicated experimental tests supplying experimental data to be compared with the numerical ones. In this way, the numerical results can be considered the reference at initial time (i.e., intact structural element). In this work, scanning LDV was used for model validation, allowing to acquire data on a dense point grid (60 DOFs were considered). On another hand, LDV-based technologies can be exploited for in-field vibrational tests, with the advantage of not being invasive (being non-contact) and not needing specific installation on the structure to be monitored, that is particularly important in case of big structures and also considering particular test scenarios (e.g., seismic/post-seismic context).

#### Acknowledgements

This research activity was carried out within the framework of the reCITY project “Resilient City – Everyday Revolution” (reCITY) – PON R&I 2014-2020 e FSC “Avviso per la presentazione di Ricerca Industriale e Sviluppo Sperimentale nelle 12 aree di Specializzazione individuate dal PNR 2015-2020”, identification code ARS01\_00592.

#### References

- [1] M. Jia, A. Komeily, Y. Wang, R.S. Srinivasan, Adopting Internet of Things for the development of smart buildings: A review of enabling technologies and applications, *Autom. Constr.* 101 (2019) 111–126. <https://doi.org/10.1016/J.AUTCON.2019.01.023>.
- [2] B. Coppola, L. Di Maio, L. Incarnato, J.M. Tulliani, Preparation and Characterization of Polypropylene/Carbon Nanotubes (PP/CNTs) Nanocomposites as Potential Strain Gauges for Structural Health Monitoring, *Nanomater.* 2020, Vol. 10, Page 814. 10 (2020) 814. <https://doi.org/10.3390/NANO10040814>.

- [3] S.A.V. Shajihan, R. Chow, K. Mechitov, Y. Fu, T. Hoang, B.F. Spencer, Development of Synchronized High-Sensitivity Wireless Accelerometer for Structural Health Monitoring, *Sensors* 2020, Vol. 20, Page 4169. 20 (2020) 4169. <https://doi.org/10.3390/S20154169>.
- [4] T.N. Tallman, D.J. Smyl, Structural health and condition monitoring via electrical impedance tomography in self-sensing materials: a review, *Smart Mater. Struct.* 29 (2020) 123001. <https://doi.org/10.1088/1361-665X/ABB352>.
- [5] M.R.P. Elenchezian, V. Vadlamudi, R. Raihan, K. Reifsnider, E. Reifsnider, Artificial intelligence in real-time diagnostics and prognostics of composite materials and its uncertainties—a review, *Smart Mater. Struct.* 30 (2021) 083001. <https://doi.org/10.1088/1361-665X/AC099F>.
- [6] K. Sugimoto, T. Sugimoto, N. Utagawa, C. Kuroda, Detection of resonance frequency of both the internal defects of concrete and the laser head of a laser Doppler vibrometer by spatial spectral entropy for noncontact acoustic inspection, *Jpn. J. Appl. Phys.* 58 (2019) SGG15. <https://doi.org/10.7567/1347-4065/AB1A2F>.
- [7] Y. Zhao, Y. Chen, L. Ye, A non-contact inspection method of tile debonding using tuned acoustic wave and laser doppler vibrometer, *J. Sound Vib.* 564 (2023) 117875. <https://doi.org/10.1016/J.JSV.2023.117875>.
- [8] E. V. Liarakos, C.P. Provdakis, Concrete damage mapping combining laser scanning vibrometry, dynamic response modeling, and ordinary kriging regression, *Mater. Des. Process. Commun.* 3 (2021). <https://doi.org/10.1002/MDP2.153>.
- [9] S. Zhao, S. Li, W. Guo, C. Zhang, B. Cong, Quantitative diagnosis method of beam defects based on laser Doppler non-contact random vibration measurement, *Measurement*. 152 (2020) 107271. <https://doi.org/10.1016/J.MEASUREMENT.2019.107271>.
- [10] M. Muramatsu, S. Uchida, Y. Takahashi, Noncontact detection of concrete flaws by neural network classification of laser Doppler vibrometer signals, *Eng. Res. Express*. 2 (2020) 025017. <https://doi.org/10.1088/2631-8695/AB8BA4>.
- [11] P. Chiariotti, M. Martarelli, G.M. Revel, Delamination detection by Multi-Level Wavelet Processing of Continuous Scanning Laser Doppler Vibrometry data, *Opt. Lasers Eng.* 99 (2017) 66–79. <https://doi.org/10.1016/J.OPTLASENG.2017.01.002>.
- [12] S.W. Doebling, C.R. Farrar, M.B. Prime, A summary review of vibration-based damage identification methods, *Shock Vib. Dig.* 30 (1998) 91–105. <https://doi.org/10.1177/058310249803000201>.
- [13] H.-P. Lin, Direct and inverse methods on free vibration analysis of simply supported beams with a crack, *Eng. Struct.* 26 (2004) 427–436. <https://doi.org/https://doi.org/10.1016/j.engstruct.2003.10.014>.
- [14] H. Jahangir, H. Hasani, M.R. Esfahani, Wavelet-based damage localization and severity estimation of experimental RC beams subjected to gradual static bending tests, *Structures*. 34 (2021) 3055–3069. <https://doi.org/https://doi.org/10.1016/j.istruc.2021.09.059>.